Pergamon

Tetrahedron 56 (2000) 1649–1653

TETRAHEDRON

Analysis of Isomerization Process of 8′-Hydroxyabscisic Acid and its 3′-Fluorinated Analog in Aqueous Solutions

Yasushi Todoroki, Nobuhiro Hirai* and Hajime Ohigashi

Division of Applied Life Sciences, Graduate School of Agriculture, Kyoto University, Kyoto 606-8502, Japan

Received 14 December 1999; accepted 21 January 2000

Abstract—8′-Hydroxyabscisic acid (8′-HOABA), the first metabolite of abscisic acid (ABA) in plants, is spontaneously isomerized to low bioactive phaseic acid (PA). We investigated thermodynamic and kinetic properties of the isomerization process in aqueous solution buffered at the various pHs, along with the effects of 3′-fluorine. The 8′-HOABA/PA ratio at equilibrium was 2:98 at 25°C, while the 3′-fluoro-8′HOABA/3′α-fluoro-PA ratio was 16:84, indicating that introduction of a fluorine at C-3′ thermodynamically reduced isomerization of 8′-HOABA to PA. The isomerization became more rapid as pH increased; the rate constant at pH 10 was higher than that at pH 3 by a factor of 2000. Introduction of a fluorine at C-3′ reduced the reaction rate by raising the activation enthalpy. This indicated that 8′-HOABA was also kinetically stabilized by the 3′-fluorine. These findings suggested that the control of pH and modification of the enone moiety of the ring would be useful to manipulate the catabolic inactivation rate of ABA.

Introduction

Abscisic acid (ABA, **1**) is the primary hormone that induces adaptive reactions to protect plants from desiccation and low temperature,[1,2] as well as for regulation of seed germination.[3] In plants, the C-8′ of **1** is hydroxylated by an 8′-hydroxylase, which has been reported to be cytochrome P450 monooxygenase,[4] to give 8′-hydroxy-ABA (**2**).[1] Metabolite **2** isomerizes to phaseic acid (**3**) with a low bioactivity before reduction to biologically inactive dihydrophaseic acid (**4**) (Fig. 1).[1] Evaluation of the biological activity of **2** is necessary to understand the inactivation process of **1**. Although the isomerization of **2** to **3** might occur enzymatically in vivo,[5] it does so spontaneously in vitro, so it has not been easy to isolate **2** without 8′-*O*-protection, much less examine its bioactivity. Zou et al.[6] and Walker-Simmons et al.[7] reported that the activities of the borate complex of **2** that dissociates in water were equivalent to those of **1** in some assays, but weaker than those of **1** in others. Thus, it was difficult to precisely estimate the net biological activities of **2**, probably because the stability of **2** in assay media was affected by factors such as pH and the temperature. Despite such uncertainty, the potency of **2** in some assays suggested that this compound would have greater activity than **3**. Another estimate of the activity of **2** was afforded by the analog 3′-fluoro-8′-hydroxy-ABA (**6**), which undergoes less isomerization than **2** (Fig. 1).[8,9] The analog **6** was sufficiently stable to be isolated without derivatization, and its activities were intermediate between those of 3′-fluoro-ABA (**5**) and 3′α-fluorophaseic acid (**7**).[8] This suggested that the activity of **2** may be also intermediate between those of **1** and **3**. These findings showed that **2** retains medium bioactivity, but loses it due to isomerization to **3**. Thus, the isomerization of **2** to **3** is a key step in the inactivation of **1**, so characterizing the isomerization of **2** to **3** is indispensable to understand the inactivation process.

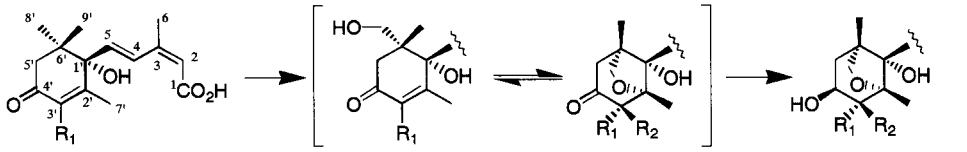

Figure 1. Metabolic inactivation pathway of **1** and **5** in plants.

Keywords: isomerization; kinetics; metabolites; enones.

* Corresponding author. Fax: +81-75-753-6284; e-mail: hirai@kais.kyoto-u.ac.jp

0040–4020/00/$ - see front matter
PII: S0040-4020(00)00068-5

The isomerization of **2** to **3** is a cyclization reaction triggered by intramolecular conjugated nucleophilic addition of the oxygen of the 8′-hydroxyl group to the electron-deficient C-2′, which is present in the β-position of the α,β-unsaturated carbonyl group. This reaction should be promoted by deprotonation of the 8′-hydroxyl group or protonation on the 4′-carbonyl oxygen. This means that the reaction rate can be affected by pH of media. In fact, **2** was more stable under acidic than alkaline conditions.[6] The electronic state of the enone moiety in the ring of **2** will also be a significant factor affecting the isomerization rate. Previously, we found that the methyl ester of **6** slowly isomerized to the methyl esters of **7** and 3′β-fluorophaseic acids (**8**).[8,9] However, quantitative analysis of the isomerization process has not been reported. In the present study, we examined the equilibrium ratios and the isomerization rates of **2**/**3** and **6**/**7** in aqueous solution buffered at various pHs and temperatures. The thermodynamic and kinetic characteristics of the isomerization process are discussed on the basis of computer-aided molecular orbital analysis of model compounds in addition to experimental results.

Results and Discussion

Preparation of 2 and 6

Precise analysis of the ^{1}H NMR spectrum of **3** showed the presence of small signals corresponding to **2** at an intensity of 1–2% of those of **3**, confirming that a methanol solution of **3** is actually a tautomeric mixture of **3** and a trace amount of **2**. Careful analysis of the methanol solution of **3** by HPLC with an ODS column revealed the existence of a small peak that eluted after **3**.[4] The compound corresponding to the peak was collected, and it showed signals similar to those of **1** on ^{1}H NMR, except the absence of the methyl protons, H_3-8′, and existence of an AB quartet at δ 3.56 and 3.70, which corresponds to the methylene protons adjacent to an oxygen atom (Table 1). This compound was partially converted to **3** on heating during concentration. Therefore, this compound was identified as **2**. The isolated **2** isomerized slowly even in acidic solutions at −20°C, so it was used for kinetic analysis of the isomerization as soon as possible after isolation by HPLC, without concentration. Metabolite **6** was isolated from a rice cell suspension culture fed with **5**.[8]

Table 1. The ^{1}H NMR signals of **1**, **2**, and **3** in methanol-d_4 (values for the chemical shifts are in δ (ppm), and those for the coupling constants in parentheses are in J (Hz)

H	**1**	**2**	**3**
2	5.74 (*s*)	5.84 (*s*)	5.79 (*s*)
4	7.77 (*dd*, 16.2, 0.6)	7.56 (*d*, 16.1)	8.10 (*d*, 16.0)
5	6.23 (*dd*, 16.2, 0.4)	5.92 (*d*, 16.1)	6.45 (*d*, 16.0)
6	2.03 (*s*)	1.94 (*s*)	1.94 (*s*)
3′	5.92 (*s*)	5.90 (*s*)	2.70 (*dd*, 18.0, 2.4)
			2.80 (*d*, 18.0)
5′	2.18 (*dd*, 16.9, 0.5)	2.37 (*d*, 17.2)	2.39 (*dd*, 18.0, 2.4)
	2.53 (*d*, 16.9)	2.48 (*d*, 17.2)	2.47 (*dd*, 18.0, 2.8)
7′	1.93 (*s*)	1.91 (*s*)	1.22 (*s*)
8′	1.06 (*s*)	3.56 (*d*, 11.1)	3.67 (*d*, 7.7)
		3.70 (*d*, 11.1)	3.95 (*dd*, 7.7, 2.8)
9′	1.03 (*s*)	1.06 (*s*)	1.01 (*s*)

It was necessary to determine the ratio of molar absorption coefficient (ε) between **2** and **3**, and **6** and **7**, to correct the isomeric ratios based on peak areas in HPLC with the UV-detector (254 nm). It would be difficult to precisely measure the absolute ratio of ε of these metabolites, especially that of the labile metabolite **2**, under these analytical conditions. So, we obtained the relative value by comparing the ratio of peak-area of the two isomers in the mixtures at the various isomeric ratios (see Experimental). The obtained relative ratio of ε at 254 nm was 1.18 for **2**/**3**, and 1.27 for **6**/**7**. Peak areas of **2** and **3**, and **6** and **7** were corrected by the relative ratio of ε to give the precise molar ratio of the each isomeric pair.

Equilibrium ratios

The metabolites **2** and **6** were incubated at three temperatures (5, 15 and 25°C; and 15, 25 and 35°C, respectively) and in eight buffer solutions (pH 3–10). After a three-week incubation, the ratio of isomers was measured by HPLC with the above relative ratio of ε. The **2**/**3** ratio was 2:98 under all pH and temperature conditions used; the free energy difference (ΔG°) was −2.3 kcal/mol. The **6**/**7**/**8** ratio changed according to temperature, but not according to pH. The isomer **8** with the axial fluorine was not found under any conditions, probably because its axial fluorine is 1,3-diaxial to the side-chain and cannot be thermodynamically labilized. The **6**/**7** ratio was 14:86 (ΔG°=−1.03 kcal/mol) at 15°C, 16:84 (ΔG°=−0.98 kcal/mol) at 25°C, and 18:82 (ΔG°=−0.92 kcal/mol) at 35°C; that is, the proportion of **6** became larger as temperature increased. Thus, the isomerization of **6** to **7** had negative entropy (ΔS°<0), which was estimated to be about −5.5 cal/mol deg if the enthalpy (ΔH°) and ΔS° were little affected by alterations in temperature. Isomerization formed the bicyclo[3.2.1]-octane ring, so the negative entropy could be attributed to a decrease in the flexibility. This must be true also of the isomerization of **2** to **3**, meaning that the **2**/**3** ratio should also be dependent on temperature. However, we found no such temperature dependency for the **2**/**3**-equilibrium ratio. If ΔS° for the isomerization of **2** to **3** was similar to that for the isomerization of **6** to **7**, then the population of **3** at 5°C should be about 1.7%, which is smaller than that at 25°C by only 0.3 points. Such a difference was too small to be detected by our HPLC analysis.

The above findings showed that the introduction of a fluorine at C-3′ stabilizes the 8′-hydroxy compound compared to the cyclized compound. We performed ab initio molecular orbital calculations in the MP2/6-311+G(d,p)//HF/6-31G(d) level, for the model reactions: ethane→fluoroethane; and ethene→fluoroethene. This substitution reaction by fluorine was more exoergic for ethene than for ethane by ca. 2 kcal/mol. This agreed with the observation that **2** was better stabilized than **3** by the C-3′ fluorine. This stabilization may have been due to delocalization of electrons or less non-bonded repulsion in sp^2 hybridization compared to sp^3.

Kinetic analysis

The isomerization rates for **2** and **6** were measured under the same conditions as the equilibrium ratios. Under all

Table 2. Rate constants (k) and activation energies of the isomerization at 25°C

pH	**2→3**				**5→6**			
	k (/s)	$\Delta G^{\ddagger}$ (kcal/mol)	$\Delta H^{\ddagger}$ (kcal/mol)	$\Delta S^{\ddagger}$ (cal/mol deg)	k (/s)	$\Delta G^{\ddagger}$ (kcal/mol)	$\Delta H^{\ddagger}$ (kcal/mol)	$\Delta S^{\ddagger}$ (cal/mol deg)
3	6.8×10^{-6}	24.5	10.6	−46.9	4.8×10^{-8}	27.6	16.2	−39.8
4	8.7×10^{-6}	24.4	11.2	−44.3	9.0×10^{-8}	27.1	17.8	−33.3
5	1.1×10^{-5}	24.2	12.2	−40.3	1.6×10^{-7}	26.8	19.9	−25.3
6	1.8×10^{-5}	23.9	12.2	−39.3	5.0×10^{-7}	26.1	20.5	−20.9
7	5.5×10^{-5}	23.3	12.4	−36.4	3.5×10^{-6}	24.9	20.0	−18.6
8	1.7×10^{-4}	22.6	17.0	−18.9	1.6×10^{-5}	24.1	21.6	−10.2
9	2.5×10^{-3}	21.0	18.9	−7.1	3.7×10^{-4}	23.6	23.5	−2.4
10	1.1×10^{-2}	19.9	16.7	−10.9	2.0×10^{-3}	21.2	20.2	−5.3

conditions examined, isomerization was observed as a first-order reaction in which the rate was proportional only to the concentration of the 8′-hydroxyl compound. As the pH and temperature increased, the reaction proceeded more rapidly. At 25°C, the half-life of **2** was 30 h at pH 3, 4 h at pH 7, and shorter than 1 min at pH 10; that is, **2** was isomerized to **3** more rapidly at pH 10 than at pH 3 by a factor of 2000. The temperature dependence of the rate was greater under alkaline conditions than under acidic conditions. The Arrhenius plots of the rate constants gave the activation energies of Arrhenius and frequency factors, which were converted to the kinetic parameters, i.e. the activation enthalpy ($\Delta H^{\ddagger}$), activation entropy ($\Delta S^{\ddagger}$) and activation free energy ($\Delta G^{\ddagger}$) (Table 2). The $\Delta H^{\ddagger}$ was higher under alkaline conditions than under acidic conditions, whereas the $\Delta S^{\ddagger}$ was negative under all conditions and its absolute value was larger under the acidic as compared to the alkaline conditions. This indicated that the slow isomerization under acidic conditions was dependent on the negative, large $\Delta S^{\ddagger}$. The transition structure under acidic conditions may be so solvated as to cause a decrease in $\Delta H^{\ddagger}$ and a rise in the absolute value of $\Delta S^{\ddagger}$. Alternatively, the reaction under acidic conditions may be associated with a concerted mechanism.

The isomerization of **6** was slower than that of **2** by a factor of 10–100 under acidic conditions and by a factor of 3–10 under alkaline conditions. This indicated that the introduction of a fluorine at C-3′ stabilized **2** kinetically in addition to thermodynamically. The pH-dependence of the isomerization rate of **6** was similar to that of **2**; at 25°C, the reaction rate constant at pH 10 was 50000-fold larger than that at pH 3. At the same pH, the $\Delta H^{\ddagger}$ of the isomerization of **6** was higher than that of the isomerization of **2**, while the absolute value of the negative $\Delta S^{\ddagger}$ of the isomerization of **6** was smaller than that of **2**. This meant that the slow reaction of **6** was caused by an increase of the $\Delta H^{\ddagger}$, unlike that in low pH solution. This suggested a decrease in solvation at the transition state of **6**/**7** isomerization. However, a better explanation would be less interaction between the 2′-carbon and 8′-oxygen of the transition state of **6**/**7** isomerization compared to **2**/**3** isomerization. This was examined by computer-assisted calculations for the model compounds.

Table 3. Mulliken charges of the heavy atoms in **11** and **12** (calculated in the MP2/6-31G*//HF/3-21G*)

Compound	C-2′	C-3′	C-4′	O-4′
11	−0.142	−0.278	0.533	−0.554
12	−0.254	0.383	0.484	−0.518

Introducing a fluorine into the conjugated system should have a large effect on the charge distribution. The fluorine at C-3′ can push the electrons of C-3′ to C-2′ by the electron-donating effect, which is attributed to repulsion between the π-electron at C-3′ and the electrons of the outermost shells of the fluorine atom, and also withdraw those of the 4′-carbonyl by the inductive effect. In addition, the fluorine itself will significantly affect polarity of the molecule. In the equilibrium state, these effects of fluorine are observed experimentally by the shifts of ^{13}C NMR signals[10] and theoretically by the atomic charges calculated by Mulliken population analysis.[11] Our previous study revealed that the ^{13}C signals corresponding to C-2′ and C-4′ in **5** were shifted toward a higher field compared to those in **1**, while C-3′ in **5** was shifted toward a lower field compared to that in **1**.[9] This indicated that introduction of a fluorine at C-3′ in **1** or **2** increased the electron density at C-2′ and C-4′ and decreased that of C-3′. The charges of the atoms corresponding to C-2′, C-3′, C-4′ and O-4′ in **2** and **6** were estimated using the model compounds **11** and **12** at the MP2/6-31G* level (Table 3). The results indicated that the charges of C-2′ and C-4′ in **6** were shifted toward negative compared to those of **2**, while those of C-3′ and O-4′ in **6** were shifted toward positive compared to those of **2**, in agreement with the ^{13}C shifts observed. The increase in the negative charge at C-2′ will result in the larger filled-orbital-filled-orbital repulsion for a nucleophile. The repulsion between C-2′ and O-8′ can be represented by the small overlap population which is calculated in the transition state, so we simulated the nucleophilic addition of a methoxide to models **11** and **12** (Fig. 2). The calculated overlap population, 0.105, between the 2′-carbon of **11** and the oxygen of methoxide in the transition-state structure was smaller than that for **12** (0.080), as expected. These results suggested that the slow isomerization of **6** is dependent on the electron-donating effect on C-2′ by the 3′-fluorine via C-3′.

Here, we demonstrated that introduction of a fluorine at C-3′ of **2** can stabilize the 8′-hydroxyl compound kinetically as well as thermodynamically. The control of pH and the

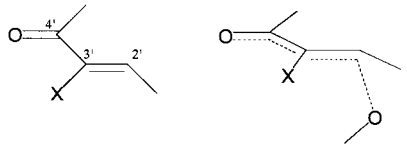

Figure 2. Model compounds **11** (X=H) and **12** (X=F), and the nucleophilic addition of a methoxide to those.

modification of the enone moiety of the ring will be useful to manipulate the catabolic rate of ABA.

Experimental

General procedures

^{1}H NMR spectra were recorded with TMS as an internal standard using a Bruker ARX500 (500 MHz) apparatus. For clarity, the conventional ABA numbering system was used to assign the peaks in the ^{1}H NMR spectra. The carbon corresponding to that of ABA in the model compounds **11** and **12** was represented by the same number as that of ABA.

Preparation of 2, 3, 6 and 7

The natural metabolite **3** (3 mg) was prepared by hydrolysis of the β-hydroxy-β-methylglutaryl ester of 8′-hydroxy-ABA isolated from immature seeds of *Robinia pseudacacia*,[12] and analyzed by HPLC with an ODS column YMC AQ-311, 6 i.d.×100 mm (solvent: 45% MeOH in 0.1% aqueous AcOH at 1.0 ml min^{-1}; detection: 254 nm). After **3** eluted at t_R 5.9 min, a compound corresponding to a small peak of t_R 7.2 min was collected, and concentrated for identification to give a mixture (30 μg) of **2** and **3** in a ratio of 70:30. Signals of **2** in the ^{1}H NMR spectrum (500 MHz, CD_3OD) are shown in Table 1. Compounds **6** (0.6 mg) and **7** (0.2 mg) were prepared by feeding **5** (4.8 mg) to suspension cultures of rice cells.[9] For isomerization examination, **2** and **6** were collected as eluates by HPLC (40% MeOH for **2** and 45% MeOH for **6**, respectively, in 0.1% aqueous AcOH) in a flask cooled to −20°C, and the solution was preserved below −20°C before incubation. The concentrations of **2** and **6** in the solutions were 35.4 and 49.1 μM, respectively. The isomeric purity was always measured by HPLC analysis just before incubation because **2** was converted to its tautomeric isomer **3** even at −20°C, although **6** has never isomerized under these conditions. The isomeric purity was 98.8–89.6% for the solution of **2** and 100% for that of **6**.

Incubation of 2 and 6 at various pHs

Buffer solutions used were 10 mM citric acid-20 mM Na_2HPO_4 for pH 3–8, and 10 mM NH_3–NH_4Cl for pH 9 and 10. The initial pHs of buffers were adjusted by considering the addition of the sample solution containing 0.1% AcOH and the incubation temperature. The sample solutions (20 μl each) were added to 180 μl of the buffer solution. Incubation was performed at 5, 15 and 25°C for **2**, and at 15, 25 and 35°C for **6**. Five-microliter aliquots were analyzed by HPLC with the ODS column (solvent: 45% MeOH in 0.1% aqueous AcOH at 1.0 ml min^{-1}; detection: 254 nm) at appropriate intervals according to the isomerization rate, and areas of the peaks of **2** and **3**, and of **6** and **7** were measured. The **2**/**3** and **6**/**7** ratios of areas obtained were converted to the corresponding ratios of concentrations by considering the ratios of molar absorption coefficients (ε), which were obtained by comparing the peak-areas of the two isomers in sample solutions of various isomeric ratios as follows. The total amount of isomers was constant regardless of their ratio, so the relative ratio (p) of ε could be obtained by solving the following equation:

$$p=(A_x-A_y)/(B_y-B_x)$$

where A_x and B_x are the areas of the isomer A and B in sample x, respectively, and A_y and B_y are the areas of the isomer A and B in sample y, respectively. The experiment for obtaining the equilibrium ratio was repeated five times, and the mean value was adopted. The standard errors were less than 0.3 point in all cases.

Kinetics and activation energies

Values for the first-order rate constant (k) of overall reaction were determined by fitting to the equation:

$$\ln [(A-Ae)/(Ao-Ae)]=-kt$$

where A is the concentration of **2** or **6** in sampled solution; Ao is the initial concentration of **2** or **6**; Ae is the equilibrium concentration of **2** or **6**; and t is the incubation time. The correlation coefficient was higher than 0.996 in all cases. The rate constants (k_1) of the reaction **2**→**3** and **6**→**7** were calculated according to

$$k_1=kK/(K+1)$$

where K is the equilibrium constant. The Arrhenius plot of k_1 at the various temperatures determined the activation energy (Ea) of Arrhenius. The correlation coefficients were higher than 0.996 in all cases. The activation enthalpy ($\Delta H^{\ddagger}$) was calculated according to

$$\Delta H^{\ddagger}=Ea-RT$$

where R is the gas constant; and T is the temperature. The activation entropy ($\Delta S^{\ddagger}$) was calculated according to

$$\Delta S^{\ddagger}=R \ln (Ah/ek_BT)$$

where A is the frequency factor obtained by the Arrhenius plot; h is the Planck constant; e is the base of natural logarithm; and k_B is the Boltzman constant. The activation free energy ($\Delta G^{\ddagger}$) was calculated according to

$$\Delta G^{\ddagger}=\Delta H^{\ddagger}-T\Delta S^{\ddagger}$$

Computational methods

The free energy difference of the model reactions, ethane→fluoroethane and ethene→fluoroethene were calculated using the Gaussian 98 (Revision A.3).[13] The lowest-energy geometries were obtained in the HF/6-31G(d) level, and characterized in the MP2/6-311+G(d,p) level.

The equilibrium geometries of models **11** and **12** were optimized in the HF/3-21G* level using PC SPARTAN Pro (ver.1.01).[14] The chemical properties for the optimized geometries were calculated in the MP2/6-31G* level using the Gaussian 98. The transition state geometries of the model reactions were determined and optimized employing minimum energy path calculations in the HF/3-21G* level using PC SPARTAN Pro. A single imaginary frequency was found for each calculation of transition states. The geometries obtained were characterized in the MP2/6-31G* level using the Gaussian 98.

Acknowledgements

This research was supported by a Grant-in-Aid (Biocosmos program) from the Ministry of Agriculture, Forestry and Fisheries of Japan (BCP-99-I-A-1).

References

1. Hirai, N. *Abscisic acid*; In *Comprehensive Natural Products Chemistry*, Mori, K. Ed.; Pergamon Press: Oxford, 1999; 8, pp 72–91.
2. Leung, J. *Annual Review of Plant Physiology and Plant Molecular Biology* **1998**, *49*, 199.
3. Yoshioka, T.; Endo, T.; Satoh, S. *Plant and Cell Physiology* **1998**, *39*, 307.
4. Krochko, J. E.; Abrams, G. D.; Loewen, M. K.; Abrams, S. R.; Cutler, A. J. *Plant Physiology* **1998**, *118*, 849.
5. Milborrow, B. V.; Carrington, N. J.; Vanghan, G. T. *Phytochemistry* **1988**, *27*, 757.
6. Zou, J.; Abrams, G. D.; Barton, D. L.; Taylor, D. C.; Pomeroy, M. K.; Abrams, S. R. *Plant Physiology* **1995**, *108*, 563.
7. Walker-Simmons, M. K.; Holappa, L. D.; Abrams, G. D.; Abrams, S. R. *Physiologia Plantarum* **1997**, *100*, 474.
8. Arai, S.; Todoroki, Y.; Ibaraki, S.; Naoe, Y.; Hirai, N.; Ohigashi, H. *Phytochemistry* **1999**, *52*, 1185.
9. Todoroki, Y.; Hirai, N.; Ohigashi, H. *Tetrahedron* **1995**, *51*, 6911.
10. Breitmaier, E.; Voelter, W. Carbon-13 NMR Spectroscopy, VHC Verlagsgesellschaft: Weinheim, 1987.
11. Mulliken, R. S. *Journal of Chemical Physics* **1955**, *23*, 1833. See also 1841, 2338, 2343.
12. Hirai, N.; Fukui, H.; Koshimizu, K. *Phytochemistry* **1978**, *17*, 1625.
13. Gaussian 98, Revision A.3, Frisch, M. J.; Trucks, G. W.; Schlegel, H. B.; Scuseria, G. E.; Robb, M. A.; Cheeseman, J. R.; Zakrzewski, V. G.; Montgomery, Jr., J. A.; Stratmann, R. E.; Burant, J. C.; Dapprich, S.; Millam, J. M.; Daniels, A.D.; Kudin, K. N.; Strain, M. C.; Farkas, O.; Tomasi, J.; Barone, V.; Cossi, M.; Cammi, R.; Mennucci, B.; Pomelli, C.; Adamo, C.; Clifford, S.; Ochterski, J.; Petersson, G. A.; Ayala, P. Y.; Cui, Q.; Morokuma, K.; Malick, D. K.; Rabuck, A. D.; Raghavachari, K.; Foresman, J. B.; Cioslowski, J.; Ortiz, J. V.; Stefanov, B. B.; Liu, G.; Liashenko, A.; Piskorz, P.; Komaromi, I.; Gomperts, R.; Martin, R. L.; Fox, D. J.; Keith, T.; Al-Laham, M. A.; Peng, C. Y.; Nanayakkara, A.; Gonzalez, C.; Challacombe, M.; Gill, P. M. W.; Johnson, B.; Chen, W.; Wong, M. W.; Andres, J. L.; Gonzalez, C.; Head-Gordon, M.; Replogle, E. S.; Pople, J. A.; Gaussian, Inc., Pittsburgh PA, 1998.
14. PC Spartan pro, version 1.01, Wavefunction, Inc., Irvine CA, 1999.